Aalborg Universitet

Integration and Decentralized Control of Standalone Solar Home Systems for off-grid Community Applications

Mashood Nasir[1], Muhammad Anees[1], Hassan A. Khan[1], *Member, IEEE*, Irfan Khan[2], *Member, IEEE*, Yinliang Xu[3], *Member, IEEE*, and Josep M. Guerrero[4], *Fellow, IEEE*

1. *SBASSE, Lahore University of Management Sciences, Pakistan, {mashood.nasir, muhammad.anees, hassan.khan}@lums.edu.pk*
2. *Marine Engineering Techn. Department Texas A&M University Galveston TX USA, irfankhan@tamu.edu*
3. *Tsinghua-Berkeley Shenzhen Institute China, xu.yinliang@sz.tsinghua.edu.cn*
4. *Department of Energy Technology, Aalborg University, Denmark, joz@et.aau.dk*

Abstract – **Photovoltaic solar home systems provide a cost-effective solution for the limited electrification of remote off-grid communities. However, due to their standalone nature, the benefit of usage diversity cannot be extracted. In this work, we present the power electronic interface along with the decentralized control scheme for the integration of standalone solar home systems for driving community load applications. Power electronic interface consists of an isolated boost converter capable support DC bus integration, thereby it formulates a DC microgrid through the interconnection of multiple standalone solar home systems. Power aggregation is achieved through decentralized controlled resource sharing based upon the resource availability and installed capacity in the individual solar home system. To ensure cost affordability and to avoid the deployment of any communication infrastructure, modified *I-V* droop control is designed for the intended application. Thereby, power aggregation through the proposed power electronic interface and its decentralized control allows us to extract the benefit of usage diversity and drive high power community power loads at a village scale. The overall schematic is simulated using MATLAB and scaled down model is implemented on hardware. Results of power aggregation from various resource sharing scenarios are illustrated.**

Index Terms— **DC Microgrid, droop Control, Rural Electrification, Solar Home System.**

NOMENCLATURE

The notation used throughout the paper is stated below for a quick reference. Other symbols are defined as required.

A. Indexes

t	Instant of time ranging from 1 to T.
i	SHS number ranging from 1 to N.

B. Parameters

N	Number of solar home systems (SHS) in the village.
P_i^{PV}	PV power generated by i^{th} SHS (W).
I_i^{PV}	PV current generated by i^{th} SHS (A).
P_i^{HL}	Local load power demand of ith SHS (W).
I_i^{HL}	Local current demand of ith SHS (A).
P_i^{CL}	Power contribution of ith SHS towards communal load demand (W).
I_i^{CL}	Current contribution of ith SHS towards communal load demand (A).
I_i^{max}	Maximum allowable current contribution of ith SHS towards communal load demand (A).
P^{CL}	Total communal load demand (W).
V^{NL}	No load reference voltage of the DC bus (V).
V^{DC}	Voltage of the DC bus (V).
V^L	Minimum allowable voltage of the DC bus (V).
V_i^b	Battery and household load bus voltage (V).
SOC_i	State of charge of the battery for i^{th} SHS (%).
SOC^0	Initial state of charge of the battery (%).
SOC_i^{min}	Minimum allowable battery state of charge (%).
SOC_i^{max}	Maximum allowable battery state of charge (%).
G_i^d	Virtual droop conductance for the interfacing converter of ith SHS (Ω^{-1}).
G_i^d	Modified droop conductance for i^{th} SHS (Ω^{-1}).
C_i	Battery capacity for i^{th} SHS (Ah).
C^{max}	Maximum available battery capacity (Ah).
α	Power-sharing speed coefficient.
I_i^{ref}	Reference current for i^{th} interfacing converter.
d_i	duty cycle of ith interfacing converter.
k_p	Proportional control coefficient for PI controller.
k_i	Integration control coefficient for PI controller.

C. Acronyms

PV	Photovoltaic
SOC	State of Charge
SHS	Solar Home System
MPPT	Maximum Power Point Tacking

I. INTRODUCTION

International energy agency (IEA) estimates that over 14 percent of the world's population (approx. 1 billion people) is living without access to electricity and 83 % of them reside in rural areas [1]. Access to electricity is the key to improve their standard of living and also a sustainable development goal (SDG) of united nations (UN) [2, 3]. SDG-7 aims to provide universal access to electricity by 2030 [4]. However, universal access to electricity is highly unlikely to be

Alternatively, Solar photovoltaic (PV) systems are becoming very popular to electrify remote rural areas with either standalone systems [5] or low power DC microgrids [2]. However, low power provisions (light(s), mobile charging and in some cases fans) are not a major success in improving the socio-economic uplift of a country [6-8]. While, large high-power microgrids are unviable due to upfront capital investment requirements [9], it is therefore important to allow aggregation of power for low cost granular solar home systems (SHS) to aggregate power to run larger communal loads such as water pumping and filtration plants or basic health units or computing resources for village schools.

Numerous standalone PV based SHS have been installed in the developing regions. Infrastructure development company (IDCOL) by Govt. of Bangladesh reports that over 4.2 million SHS have already been installed with a target of 6 million by 2021 [10, 11]. A similar effort has been done in Pakistan under Chief Minister Ujala Scheme in Punjab, where students of backward areas are provided with standalone solar systems for DC lights and fans [9]. Similarly, there is a number of other initiatives for rural electrification in India and other countries [11-13]. While a large number and types of these systems are available, there is no mechanism to maximize the power utilization through sharing and taking advantage of usage diversity at a neighborhood level.

In this work, we propose a power electronic interface and decentralized control mechanism based on modified *I-V* droop method utilizing the battery state of charge (incorporating local solar PV generation and load requirements) and battery capacity to allow power-sharing at SHS level which could be used for a higher power communal application. We further develop the hardware to verify power-sharing scenarios. This work will, therefore, be very important in allowing power aggregation from tens of millions of standalone SHS with the provision of power aggregation for the benefit of many rural communities.

Qobad *et al.*[14] presented a SOC based modified droop control for resource sharing in multiple DC microgrids. Similarly, Xiaonan *et al.* [15] developed an adaptive dual loop droop control (inner current loop and outer voltage loop) on the basis of the state of charge (SOC) balancing for distributed storage resources in DC microgrids. However, both of these schemes use dual-loop *V-I* control with two PI controllers, where the inner loop is responsible for controlling the current and outer loop is responsible for voltage stabilization. Due to the delays associated with dual-loop control, response time and dynamic performance of the scheme is compromised. Alternately, in this work, we have employed *I-V* droop control utilizing an inner current loop only, which has proven better dynamic performance and lower response time as compared to the *V-I* droop [16].

Mashood *et al.* [17] presented an adaptive controller based upon modified droop using *I-V* droop characteristics. However, in [17], the droop was modified in accordance with the battery SOC index only. The battery capacity (Ah), which is an important factor for deciding power contributions to community loads was not considered in [17]. Alternatively, in this work, we have modified the droop coefficient based upon both, SOC of the battery as well as its installed capacity. Considering both these factors while deciding power contributions for the community loads enables a proportionate and natural resource balancing at a village scale. Moreover, IV droop control with only one current loop exhibits a fast response in case of varying communal load demands as exhibited through simulations and hardware results.

The rest of this paper is organized as follows. In Section II, the power electronic interface for the formulation of DC microgrid through the DC bus interconnection of multiple SHS is presented. In Section III, decentralized control based upon the modified droop scheme is presented. Section IV presents simulation and hardware results for various possible power pooling scenarios at varying communal load demands. Based upon the results and discussions a conclusion is drawn in section V.

II. POWER ELECTRONIC INTERFACE FOR THE INTEGRATION OF MULTIPLE STANDALONE SOLAR HOME SYSTEMS

Consider the scenario of a remotely located village where national grid interconnection is not available. Due to the unavailability of national grid interconnection, a large number of solar photovoltaic (PV) based standalone solar home systems (SHS) have been installed by individual households to cater the basic needs of lighting, heating, cooling, and mobile phone charging. The configuration of a typical SHS along with the power electronic interface required for the integration of multiple SHS is shown in Fig. 1. A typical SHS consists of a roof-mounted PV panel, a battery storage system and a DC/DC converter based battery charge controller for the optimal extraction of incident solar energy through maximum power point tracking (MPPT). Generally, the battery voltage is relatively lower than the PV output voltage, therefore, a buck converter is employed for lowering down PV panel voltages. Various MPPT techniques are used for the extraction of maximum power from incident solar energy, however, perturb and observe (P&O) method is largely used in typical solar home systems due to its simplicity and low computational complexity [18]. The algorithm processes PV panel voltage and current to generate the duty cycle of the buck converter ensuring maximum power extraction from the PV panel at a given solar irradiance [18].

The ideal energy balance model (neglecting the losses associated with converter and battery) of a SHS working in isolation is given by (1) [17]. The losses associated with the operation of SHS mainly include losses due to charging/discharging of the battery, power electronic conversion losses and the distribution losses of the electrical

power [7, 19]. Since these losses mainly affect the overall efficiency of the operation without significantly affecting the control parameters, therefore, for the simplicity of the analysis, these losses are neglected for the purpose of control design. Therefore, ideal energy balance states that the net power generated by PV panels P^{PV} in the time interval Δt is used for battery charging and fulfilling household demand P^{HL}. When incident solar irradiance and associated PV power generation is zero, the battery is discharged to fulfill the household demand.

$$P^{PV}\Delta t = P^{HL}\Delta t + \int_0^T V^b \left(I^{PV} - I^{HL} \right) dt \tag{1}$$

Where, V^b is the voltage level of the bus at which battery and household loads are connected, I^{PV} is the net current generated by PV panel after DC/DC conversion and I^{HL} is the current demand by the household load. The net energy entering and leaving from the terminals of the battery is accounted in term of its state of charge (SOC) through Coulomb counting method [20], and is given by (2), where SOC_0 is the initial value of battery SOC and C is the rated capacity (Ah) of the battery.

$$SOC = SOC^0 + \frac{1}{C}\int_0^T \left(I^{PV} - I^{HL} \right) dt \tag{2}$$

On a village scale, there are multiple SHS working in isolation and in the existing configuration, there is no mechanism to aggregate electricity for community load applications. For instance, during the day time, incident solar irradiance is generally high and due to plenty of sunshine, lighting load demand is minimal, thereby surplus power generated by SHS may undergo wastage due to the limited storage size. Alternately, this surplus power can be utilized for community applications if there exists a mechanism for power pooling through which multiple SHS can contribute together for community loads The aggregated power from multiple SHS may be utilized by the village school load, water pumping load as well as the hospital load of the village. This provision of community loads in low power SHS based village electrification schemes [6, 8], or even low-power, low-voltage DC microgrids based electrification schemes is otherwise unsustainable due to the higher distribution losses and dedicated generation requirements [19, 21].

The power electronic interface required for the realization of such an aggregation with simplified control and minimal infrastructural requirements is proposed and is shown in Fig. 1. Power electronic interface consists of a DC-DC converter at each SHS along with a DC bus interconnection for the common coupling of multiple SHS. The integration of multiple SHS is achieved via DC bus interconnection, thereby, the proposed interface in conjunction with the existing SHS formulates a village scale DC microgrid. The proposed retrofitting interface thus formulates a swarm of energy in which energy can be pooled from multiple SHS for the community loads connected to the DC bus.
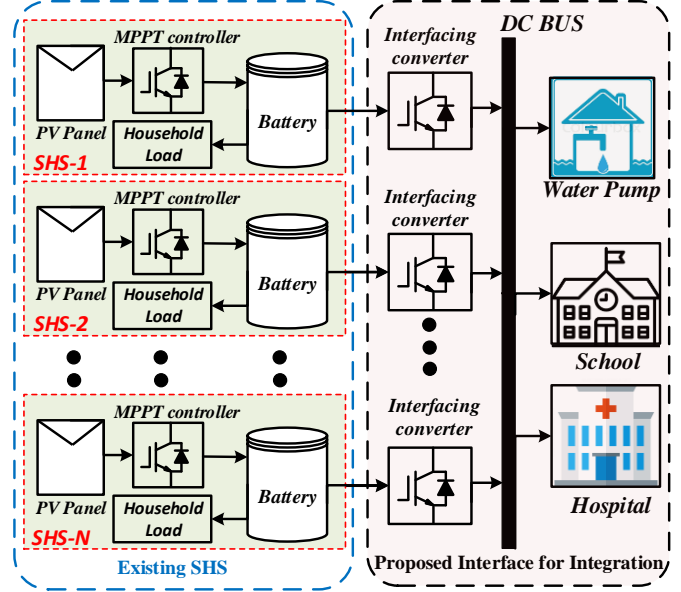

Fig. 1. Existing village electrified via solar home systems (SHS) and the proposed power electronic interface required for their integration through DC bus interconnection

For a village having N SHS operating in the swarm mode (as shown in Fig.1), the communal load demand P^{CL} is fulfilled through the power contributions from individual SHS P_i^{CL} represented in terms of individual current contributions I_i^{CL} from the battery of ith SHS and household bus voltage V_i^b given by (3).

$$P_i^{CL} = V_i^b I_i^{CL} \tag{3}$$

$$P^{CL} = \sum_{i=1}^N P_i^{CL} = \sum_{i=1}^N V_i^b I_i^{CL} \; ; \; 0 \le I_i^{CL} \le I_i^{\max} \tag{4}$$

Where I_i^{max} is the maximum allowable current contribution from an individual household depending upon the discharge rating of the battery specified by the battery manufacturer. As a result of communal load sharing, ideal energy balance at each SHS is modified and is given by (5). Similarly, resource availability index, i.e. SOC_i is also modified due to communal load sharing and is given by (6).

$$P_i^{PV}\Delta t = P_i^{HL}\Delta t + \int_0^T V_i^b \left(I_i^{PV} - I_i^{HL} - I_i^{CL} \right) dt \tag{5}$$

$$SOC_i = SOC_i^0 + \frac{1}{C}\int_0^T \left(I_i^{PV} - I_i^{HL} - I_i^{CL} \right) dt \tag{6}$$

Where, i subscript denotes the SHS number in the village, SOC^0 is the initial state of charge of the battery with the rated capacity of C (Ah), I^{PV} is the time-varying current produced by the PV panel after the processing of MPPT converter, I^{HL} is the time-varying household load demand and I_i^{CL} is the current contribution from SHS battery to pool for the communal load demand.

Since communal loads are connected to DC bus through a distribution conductor, therefore distribution losses are associated with the delivery of power from DC bus to communal loads. It has been shown in [7] that significantly higher distribution efficiency (higher than 99%) can be achieved using higher voltage level and thick conductor size. Moreover, losses associated with the distribution of power does not directly impact the control parameters, therefore, power distribution losses are considered negligibly small and neglected for the purpose of proposed control design in this study. DC bus voltage V^{DC} is generally kept higher from household bus voltage level V^b. Therefore, the interfacing DC/DC converter between the battery of an individual SHS and coupling DC bus must be capable to perform the desired boost operation (from V^b to V^{DC}) along with maintaining the voltage of DC bus within the specified range of operation. Moreover, for reliable operation, the grid side needs to be isolated from SHS, therefore, an isolated boost converter is required at each interfacing SHS.

Power electronic circuit diagram along with control flow algorithm for i^{th} interfacing isolated boost converter has been shown in Fig. 2. For the maximum allowable ripple ΔI_L in the current and the maximum allowable ripple ΔV_c in the output voltage of isolated boost converter, the value of inductor L, capacitor C, and DC voltage gain can be calculated through (7) to (9) at a given switching frequency f_{sw} and associated time period T_s. These calculations are based upon volt-sec and amp-sec balance assuming that converter is operating in continuous conduction mode (CCM) [22].

$$L = \frac{V^b dT_s}{2\Delta I_L} \tag{7}$$

$$C = \frac{V^{DC} dT_s}{2R\Delta V_c} \tag{8}$$

$$\frac{V^{DC}}{V^b} = \frac{n}{1-d} \tag{9}$$

Where, n is the turn ratio of the transformer and d is the duty cycle of the converter calculated through the proposed control algorithm discussed in detail in the next section. Since there are four MOSFETs (Q1, Q2, Q3, and Q4) in the power electronic circuit of isolated boost converter, therefore, their on and off times are calculated based upon d in a switching time period T_s and are summarized in table I.

<div align="center">
TABLE I
SWITCHING TIMES FOR THE MOSFETs OF INTERFACING ISOLATED BOOST CONVERTER
</div>

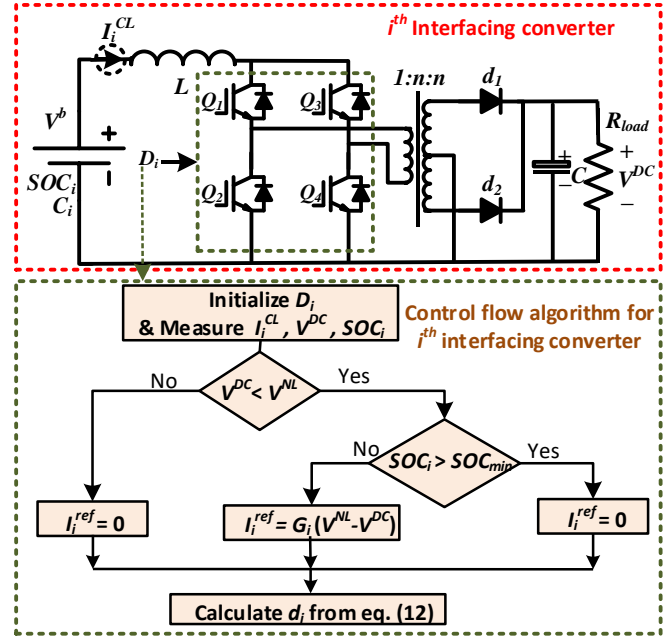| Switches	dT_s	$(1-d)T_s$	dT_s	$(1-d)T_s$
Q1	ON	ON	ON	OFF
Q2	ON	OFF	ON	ON
Q3	ON	ON	ON	OFF
Q4	ON	OFF	ON	ON

Fig. 2. Power electronic circuit and control flow algorithm for interfacing isolated boost converter.

III. DECENTRALIZED CONTROL SCHEME FOR COORDINATED POWER POOLING

The integration of multiple SHS through the proposed power electronic interface formulates a village scale DC microgrid with spatially distributed generation and storage resources. The coordination among the spatially distributed resources in various SHS is achieved through the decentralized control of the interfacing boost converter. The overall control objective is to keep the voltage stable at the interfacing DC bus while controlling power contributions from individual SHS such that each house contributes according to its resource availability as well as installation capacity and this coordination is achieved without any physical communication layer among multiple SHS. Ideally, the SHS with higher resource availability and higher installed capacity should contribute more to the community load application, in comparison to the SHS with relatively lower resource availability and lower installed capacity.

A. Modified I-V Droop Control Scheme

For the ith SHS in the system, the interfacing converter decides its power contribution P_i^{CL} for the community load application based upon the modified I-V droop control scheme as shown in Fig. 3. A typical I-V droop controlled microgrid enables power sharing from multiple sources interfaced through parallel connected converters [16]. The power-sharing from individual sources can be controlled in proportion the droop conductance G^d of the interfacing converters such that a higher value of G^d increases the power contribution from the source, while a lower value of G^d reduces the power contribution [16]. Since there is no physical communication layer among multiple SHS, so the

adaptive droop scheme and associated contributions solely rely upon the local information of SHS. In this work, droop conductance G_i^d is modified according to a) SHS resource availability, b) SHS installed capacity and c) DC bus voltage.

The resource availability of ith SHS can be quantified in terms of its state of charge SOC_i given by (6). However, different SHS across a village may have different installed capacities of PV generation and battery storage. From (6), it can be seen that the way SOC_i is defined, it is normalized over individual battery capacity C_i. Therefore, it accounts for variations in PV generation but it does not account for variations in the installed battery capacity. Therefore, the installed capacity of ith SHS can be quantified in terms of the battery capacity C_i (Ah). Mashood et al. [17] presented the idea of SOC based modified droop for the decentralized control of multiple DC nanogrid clusters in a village electrification scenario, however, the possible dependence of resource sharing on the battery capacity C_i was not evaluated. The idea here is to adjust power contributions such that an individual SHS may contribute to the community load based upon its resource availability SOC_i as well as installed capacity C_i. Since the very first priority of every SHS is to fulfill its local load demand P_i^{HL}, therefore, based upon the household load profile, a minimum storage threshold SOC_i^{min} can be defined below which i^{th} household cannot participate for community power pooling. Therefore, only those SHS having $SOC_i > SOC_i^{min}$ can participate for community resource pooling. An adaptive droop coefficient G_i as a function of resource availability index SOC_i, and installed capacity index C_i is defined and is given by (10).

$$G_i = \frac{C_i}{C_{max}} G_i^d \left(\frac{SOC_i - SOC_i^{min}}{SOC_i^{max} - SOC_i^{min}} \right)^\alpha ; \forall i \in [1, N] \quad (10)$$

Where i subscript denotes the SHS number out of N connected SHS, G^d is the virtual droop conductance based upon the power ratings of the interfacing converter, SOC_{max} is the maximum utilizable SOC of the installed battery, C_{max} is the highest battery capacity in the village and α is the speed of power sharing. A graphical representation of G_i and its dependence upon various parameters (SOC_i, C_i and α) is also pictorially represented in Figs 3. From Figure 3, it can be seen that with an increase in SOC_i or C_i, droop coefficient increases, so does the slope of the I-V curve and conductance parameter G_i. With the increase in G_i, current contribution, I_i^{CL}, and power contribution P_i^{CL} tends to increase as represented by Fig 3. Similarly, with the increase in α, power-sharing speed increases such that SOC_i of various SHS may quickly equalize their energy capacity.

At no load condition, there is no communal load demand at the DC bus, therefore, net current contribution from SHS to DC bus is zero and the voltage is fixed at V^{NL}. With the increase in communal load demand, DC bus voltage V^{DC} tends to drop and based upon the difference of V^{NL} and V^{DC}, power is transferred from SHS to DC bus for communal load fulfillment.
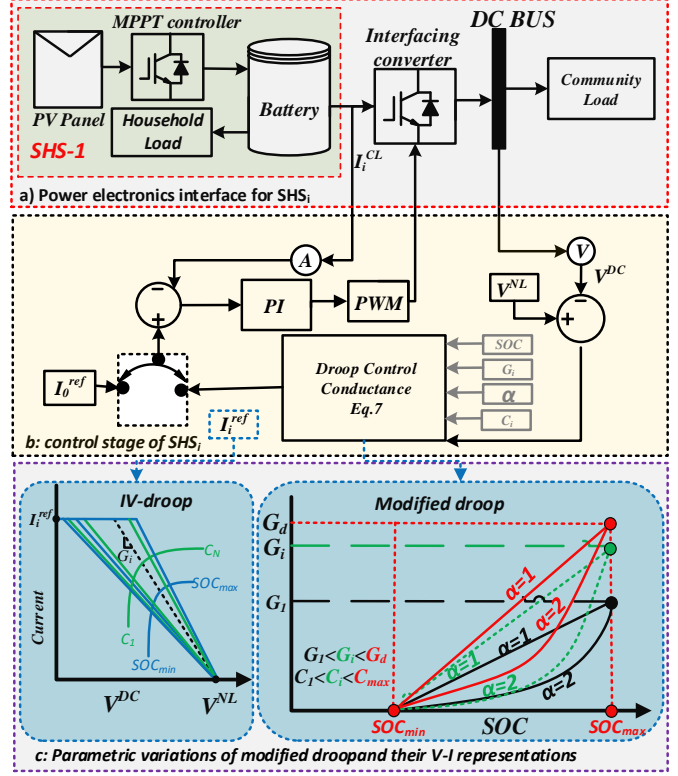

Fig. 3. Proposed Decentralized Control and droop realization for coordinated resource pooling

When load demand is excessively high and SHS contributions are insufficient to fulfill the demand, DC bus voltage tends to decrease more than the desired allowable limit V^L and therefore, an excessive load is shut down with the help of an under voltage relay. Generally, a variation of 5% is allowed in DC bus voltage [7]. Within the allowable voltage limit, i.e. $V^L < V^{DC} < V^{NL}$ the current contribution from an individual SHS is decided based upon the DC bus voltage V^{DC} and modified droop conductance G_i given by (10). A current reference I_i^{ref} is generated, which ensures that current contribution from the battery of an individual SHS is in proportion to its resource availability and installed capacity as shown by (11).

$$\begin{cases} I_i^{ref} = G_i \left(V^{NL} - V^{DC} \right); \forall i \in [1, N] \ \text{if } SOC_i > SOC_{min} \\ I_i^{ref} = 0 ; \forall i \in [1, N] \ \text{if } SOC_i \leq SOC \ min \end{cases} \quad (11)$$

As shown in Fig. 2, an inner loop current control is then used to control the output current contribution of SHS battery I_i^{CL} (also input current of the interfacing converter) through PI controller that generates the duty cycle d_i given by (10)

$$d_i = k_p \left(I_i^{ref} - I_i^{CL} \right) + k_i \int_0^t \left(I_i^{ref} - I_i^{CL} \right) dt \quad (12)$$

Where k_p and k_i are the proportional and integral constant for PI controller respectively. Their values are selected based upon the transfer function method of the isolated boost converter [22]. This duty cycle is then used to drive the isolated boost converter and associated switches as shown in

Table 1. The duty cycle d_i at each interfacing node ensures that while fulfilling communal load demand, SHS having higher resource availability SOC_i and higher battery installed capacity C_i contributes more current towards communal load demand fulfillment in comparison to SHS having relatively lower values of SOC_i and C_i. Similarly, despite having the same state of SOC_i, the battery with higher capacity should supply more current for community load application and vice versa. Since household bus voltage V_i^b does not vary significantly, therefore current contribution I_i^{CL} from i^{th} nanogrid is a direct measure of the power contribution towards communal demand fulfillment as shown by (3) and (4). Power contributions P_i^{CL} of individual SHS towards communal load demand fulfillment can be calculated in terms of I_i^{CL} and V_i^b as given by (3). This way a communication-less, yet proportionate balancing of resources at a village scale may be obtained and community benefits may be achieved [17].

IV. RESULTS AND DISCUSSIONS

In order to validate the proposed scheme, it is implemented on MATLAB/Simulink and a scaled down version is also prototyped in the laboratory. Various test cases are analyzed and the results of power-sharing at various communal demands obtained through the proposed interface and decentralized control methodology are presented. Only the results of steady-state power-sharing scenarios are presented in the current scope of the work.

A. Simulation setup and Results

The proposed power electronic interface is shown in Fig. 1 is implemented on MATLAB using the physical models of the converters, batteries and PV panels available in the sim power system library of the Simulink. The control scheme presented in Fig. 2 is applied for the decentralized resource sharing. Various parameters of the simulation case study are presented in Table II.

TABLE II
PARAMETERS OF SIMULATED CASE STUDY

Description of the Parameter	Symbol	Value
Number of SHS	N	3
Switching frequency of Converter	F_{sw}	10kHz
Rated voltage of each battery	V^b	12 V
Battery capacity for various SHS	C_i	50-100 Ah
PV capacity for various SHS	P^{PV}	200-500W
Household load capacity	P^{HL}	100-200W
Community load demand	P^{CL}	0-600 W
Max allowed current contribution	I_i^{max}	20 A
Threshold for community sharing	SOC_{min}	40 %
Max utilizable Threshold	SOC_{max}	100 %
No load voltage for DC bus	V^{NL}	48 V
Converter droop conductance	G_i^d	$(0.1\ \Omega)^{-1}$
PI Controller parameters	kp, ki	0.3, 10
DC bus Capacitance	C_{bus}	10 mF
Inductor value for boost converter	L	0.5mH
The capacitor of boost converter	C	330 µF
Transformer turn ratio	n	1

The test case scenarios are selected to highlight the dependence of the proposed control algorithm and associated power-sharing for communal load fulfillment on the state of charge SOC_i and capacity C_i of the battery. If MPPT is also kept operational, then it will be difficult to decouple the change in SOC due to MPPT, local load demand and communal load demand. Therefore, in all test case scenarios, local load demand is kept exactly equal to PV power generation and change in SOC is affected only due to power-sharing for communal load demand fulfillment. Therefore, for a better understanding of the power-sharing results, it is assumed that during simulation, PV power generation P^{PV} is equal to the household demand P^{HL}. Hence, according to the energy balance presented in (5) – (6), battery energy is being used only for fulfilling the community load demand P^{CL}. In order to visualize the effect of variations in resource availability (SOC_i) and installed capacity C_i on communal power contributions, the following three cases are simulated. Rather than considering the constant power demand at the load side, communal load demand is varied and the associated results of power contributions are observed. The communal load demand is varied according to the daily usage profile of community loads for a typical village such that at the night time, there is no communal demand. While, at the start of the day, communal demand is relatively low in comparison to its demand at the mid of the day. Therefore, community load demand pattern is divided into intervals, i.e. a) no community load, b) low demand of community load and c) high demand for community loads. These load transients are applied at 0.02 sec, 0.04 sec, 0.06 sec and 0.08 sec to observe the response of controller in case of an instant increase or decrease in load power demand. In the start, load demand is kept zero. The first transient is applied at 0.02 sec and load demand is increased from 0 W to 300 W. For the second transient at 0.04 sec, load demand is further increased from 300 W to 600 W. On the contrary, for the third transient at 0.06 sec, load power demand is decreased from 600 W to 300 W and then for the fourth transient at 0.08 sec it is further reduced to zero watt. Moreover, to have a comparative performance measure, the results of power-sharing through I-V control used in this study are compared with conventional V-I droop control in the fourth simulation scenario.

1) Case 1: SHS having same installed Capacity and different Resource Availability

Since SOC_i is a direct measure of the resource availability and C_i is the measure of the installed capacity in the ith SHS, therefore, in this scenario, power pooling is evaluated among three SHS having the same battery capacity, i.e. $C_1 = C_2 = C_3 = 100$ Ah and different resource availability, i.e. $SOC_1 = 50\ \% > SOC_2 = 60\ \% > SOC_3 = 70\%$. The results of power contributions from individual SHS P_i^{CL} and variations in DC bus voltage V^{DC} for the varying communal demand is shown in Fig. 4(a).
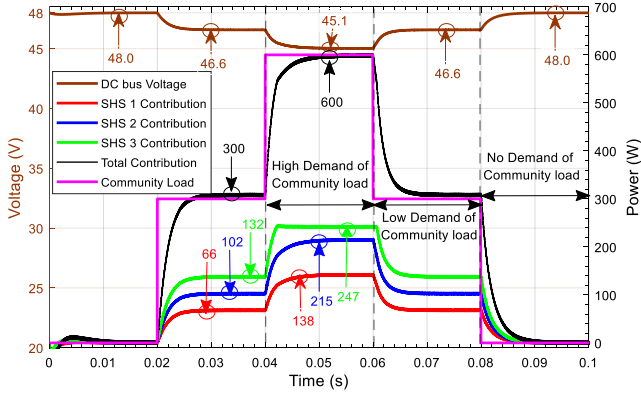
Fig. 4 (a). DC bus voltage V^{DC} profile (left Y-axis) and individual power contributions of various SHS ($P_1{}^{CL}$, $P_2{}^{CL}$, and $P_3{}^{CL}$) (right Y-axis) at varying communal load demand in case 1 (simulation results).

It can be seen from the figure that with the increase in communal load demand, V^{DC} tends to drop down, as a result of which power contributions from various SHS $P_i{}^{CL}$ are defined in proportion to resource availability SOC_i. Since, $SOC_1 > SOC_2 > SOC_3$, therefore, in accordance to the modified droop (given in (11) - (12) and Fig. 4), SHS 1 is supplying relatively lower power in comparison to SHS 3, which is contributing a relatively higher amount of power for community applications. For instance in Fig. 4 (a), during low demand of community load, i.e. 300W, SHS 1 contributes 66W, SHS 2 contributes 102 W and SHS 3's contribution is highest among all, i.e. 132 W. The power-sharing continues with the same proportion in high power community demand as well. Therefore, the desired objective of balancing community resources is realized using the proposed power electronic interface and decentralized control controllability such that the house having higher resource availability is contributing more towards community load applications. Variations in SOC_i with varying communal power demands and associated power contributions have been presented in Fig. 4 (b). To highlight the effect of SOC variations, accelerated simulations have been performed for one hour by scaling the SHS battery capacity.
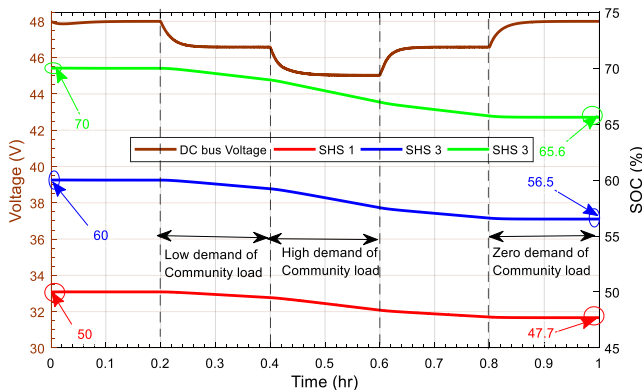

Fig. 4 (b). DC bus voltage V^{DC} profile (left Y-axis) and SOC variations of various SHS (SOC_1, SOC_2, and SOC_3) (right Y-axis) at varying communal load demand in case 1 (simulation results).

Results in Fig. 4 (b) shows that at the end of the one-hour interval, the net change in SOC is more for SHS with higher resource availability as compared to the SHS having relatively lower resource availability. For instance, the net change in SOC for three SHS is 4.4 %, 3.5 %, and 2.3% respectively, with SHS 1 being the house with highest resource availability and SHS 3 being the house with the least resource availability.

2) Case 2: SHS having the same installed capacity and same resource Availability

In order to visualize the effect of variations in installed capacity over power contributions, installed capacity and resource availability in SHS 1 is kept same as that of case 1, i.e. $C_1 = 100$ Ah and $SOC_1 = 50$ %. While, power pooling scenario is evaluated for other two SHS having same battery capacity, i.e. $C_2 = C_3 = 80$ Ah and similar resource availability, i.e. $SOC_2 = SOC_3 = 60\%$. The results of power contributions $I_i{}^{CL}$ for communal load demand fulfillment and associated changes in SOC_i are shown in Figs. 5 (a) and 5 (b) respectively.

From Fig. 5 (a) various important observations can be highlighted in terms of power contributions from the individual household. First of all, since both SHS 2 and SHS 3 have the same resource availability and installed capacity, therefore, their power-sharing is proportionate such that to fulfill low demand of community load, SHS 2 contributes 110 W, while, SHS 3 contributes 111 W. Similarly, to fulfill high demand for community load, both share 210 W and 213 W respectively. Another important observation is that despite the total communal demand pattern and SHS 1 parameters are kept the same, its power contribution is different in comparison to case 1. In case 1, SHS 1 is supplying 66 W, while in case 2 it is supplying 79 W for the fulfillment of low demand of community load. Similarly for the fulfillment of high demand of community load, in case 1 SHS 1 is supplying 138 W, while in case 2 its contribution is 157 W. This difference of power-sharing arises from the difference in DC bus voltage and compensated through high power contribution form SHS 1 as highlighted in Fig. 5 (a). Therefore, the proposed controlled methodology has the ability to modify droop conductance and associated power contributions in accordance to the varying swarm scenarios, where, different SHS may have different installed capacity and time-varying resource sharing capabilities.

Variations in SOC_i for case 2 through accelerated simulations have been presented in Fig. 5(b). Results in Fig. 5 (b) shows that at the start and at the end of the one-hour interval, both SHS 2 and SHS 3 have the same SOC i.e. the net change in SOC in both SHS is 3.7 %. Hence, the proposed modified droop control enables proportionate power-sharing in case if various SHS with identical resource availability and installed capacity pool together for community load applications.
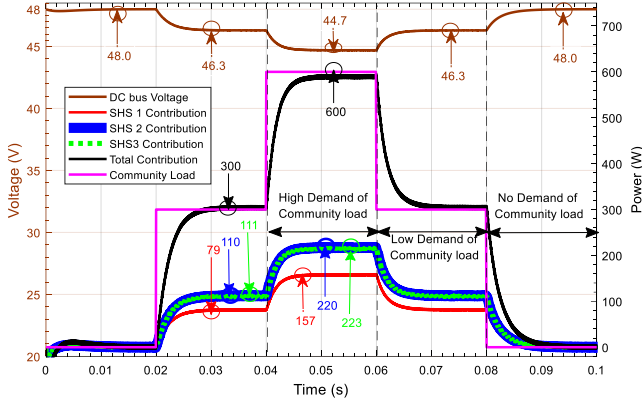
Fig. 5 (a). DC bus voltage V^{DC} profile (left Y-axis) and individual power contributions of various SHS ($P_1{}^{CL}$, $P_2{}^{CL}$, and $P_3{}^{CL}$) (right Y-axis) at varying communal load demand in case 2 (simulation results).
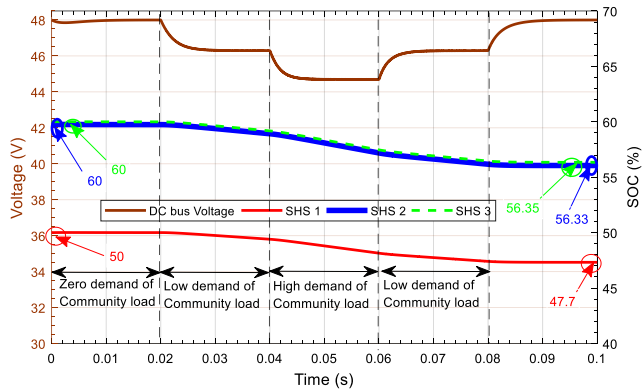

Fig. 5 (b). DC bus voltage V^{DC} profile (left Y-axis) and SOC variations of various SHS (SOC_1, SOC_2, and SOC_3) (right Y-axis) at varying communal load demand in case 2 (simulation results).

3) Case 3: SHS having the different installed capacity and same resource availability

In this scenario, installed capacity and resource availability in SHS 1 is kept the same as that of case 1 and case 2, i.e. C_1 = 100 Ah and SOC_1 = 50 %. While, power pooling scenario is evaluated for other two SHS having similar resource availability, i.e. $SOC_2 = SOC_3 = 60\%$ and different installed capacities i.e. $SOC_2 = 100$ Ah $> SOC_3 = 80$ Ah. Results of power pooling from individual households $I_i{}^{CL}$ are presented in Fig. 6. From Fig. 6, important observations can be highlighted that despite both SHS 2 and SHS 3 have the same resource availability, but they both are contributing differently to the fulfillment of communal load demand. SHS 2, due to higher battery capacity, allows more power to be shared for community applications, i.e. 120 W and 237 W for low demand and high demand scenarios, while SHS 3 allows relatively lower power to be shared for the community load applications, i.e. 104 W and 209 W for high and low demand scenarios respectively. Therefore, through the proposed modified droop method, a proportionate power-sharing based upon the installed capacity of various SHS in the village may be achieved.
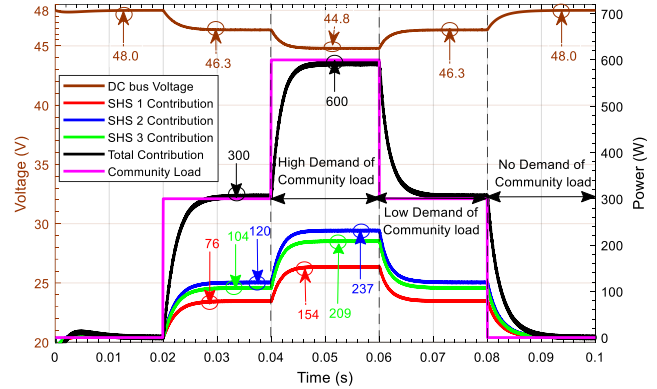

Fig. 6. DC bus voltage V^{DC} profile (left Y-axis) and individual power contributions of various SHS ($P_1{}^{CL}$, $P_2{}^{CL}$, and $P_3{}^{CL}$) (right Y-axis) at varying communal load demand in case 3 (simulation results).

4) Case 4: Comparison of IV-droop Controller with V-I Droop Control.

The results of the I-V droop controller used in the proposed scheme are compared with conventional V-I droop control strategy presented in [14, 15]. Fig. 7 shows the comparison of the proposed controller's performance in comparison to the controller presented in [14, 15]. From Fig. 7 it can be observed, that the transient response of I-V droop control including settling time and overshoot response of the proposed I-V controller is much better than V-I droop control presented in [14, 15]. As evident from Fig. 7, the proposed I-V control Exhibits faster dynamics with lower settling time (less than 0.005 sec), comparatively negligible overshoot and lower ringing in comparison to I-V droop. Although steady-state power-sharing characteristics of both of these droop realization are same, and they both converge to same power-sharing characteristics, however, their output impedance and transient characteristics are largely different, which results in different transient response and stability margins for both of the droop methods [16, 23].
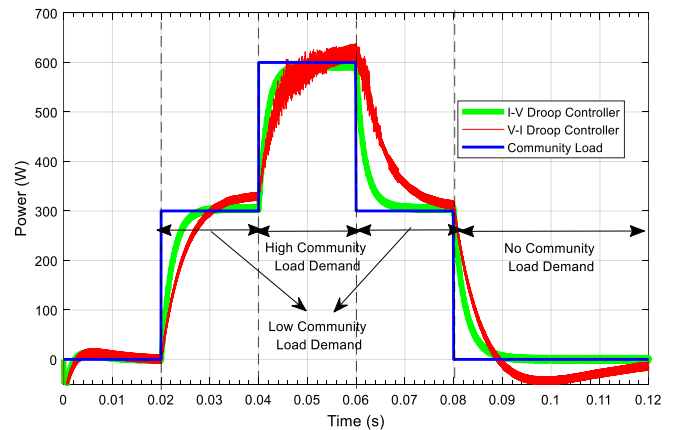

Fig. 7. Comparison of V-I droop controller power-sharing with I-V droop control power-sharing

B. Hardware setup and Results

The scaled down version of the proposed power electronic interface shown in Fig. 1 is implemented on hardware for the integration of two off-the-shelf available SHS, BBOX, bPower50 [24]. Generally, off-the-shelf solutions are available in low power ranges, i.e. up to 100 W, therefore, their high power counterparts i.e. up to 1 kW output power are also designed indigenously in the laboratory. Interfacing converters are also prototyped in the laboratory and integration is performed using the control methodology described in section II. The hardware setup for the integration of two SHS is shown in Fig. 8. Various parameters of the hardware implementation are presented in Table III. For a better understanding of the power-sharing results, household demand P^{HL} is kept exactly equal to PV power generation P^{PV}. Thereby, the effects of integrating storage elements through the proposed interface and decentralized control methodology are highlighted. In order to visualize the effect of variations in resource availability SOC_i and installed capacity C_i on communal power contributions, following three integration experiments are performed in the laboratory.
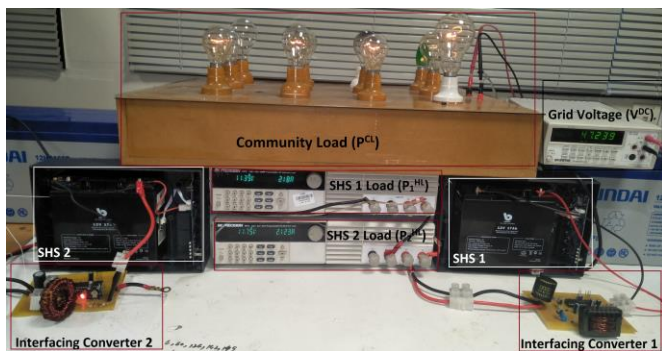

Fig. 8.   Hardware Implementation setup for the integration and decentralized control of two SHS.

TABLE III
PARAMETERS OF HARDWARE IMPLEMENTATION

Description of the Parameter	Symbol	Value
Number of SHS	N	2
Switching frequency of Converter	f_{ew}	20 kHz
Rated voltage of each battery	V^b	12 V
Battery capacity for various SHS	C_i	80-120 Ah
PV capacity for various SHS	P^{PV}	200-300W
Household load capacity	P^{HL}	50-200W
Community load demand	P^{CL}	0-150 W
Max allowed current contribution	I_i^{max}	10 A
Threshold for community sharing	SOC_{min}	40 %
Max utilizable Threshold	SOC_{max}	100 %
No load voltage for DC bus	V^{NL}	48 V
Converter droop conductance	G_i^d	$(0.1 \ \Omega)^{-1}$
Micro-controller Specifications	PIC	16F877A
DC bus capacitance	C_{bus}	3.3 mF
Inductor value for boost converter	L	0.1mH
Capacitor of boost converter	C	330 μF

1) Case 1: SHS having the same installed Capacity and different Resource Availability

In this experiment, power pooling is evaluated among two SHS having same battery capacity, i.e. $C_1 = C_2 = 120$ Ah and different resource availability, i.e. $SOC_1 = 70 \% < SOC_2 = 80 \%$. The results for power-sharing scenarios at varying community loads demand are shown in Fig. 9 (a). The results show that the SHS with higher resource availability, i.e. SHS 2 contributes more towards communal load fulfillment in both, high and low demand communal load scenarios. In order to fulfill the lower communal demand, SHS 2 is contributing 48 W and SHS 1 is contributing relatively low power i.e. 17 W. Similarly, during high power demand, SHS 2 is contributing 76 W and SHS 1 due to lower resource availability is contributing 34 W. The same effect can be observed in terms of change in SOC of the relevant SHS as shown in Fig. 9 (b).
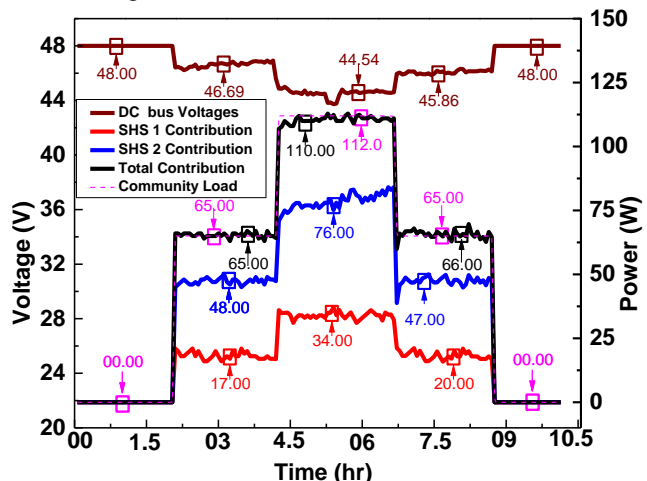

Fig. 9 (a).   DC bus voltage V^{DC} profile (left Y-axis) and individual power contributions of various SHS (P_1^{CL} and P_2^{CL}) (right Y-axis) at varying communal load demand in case 1 (Hardware results).
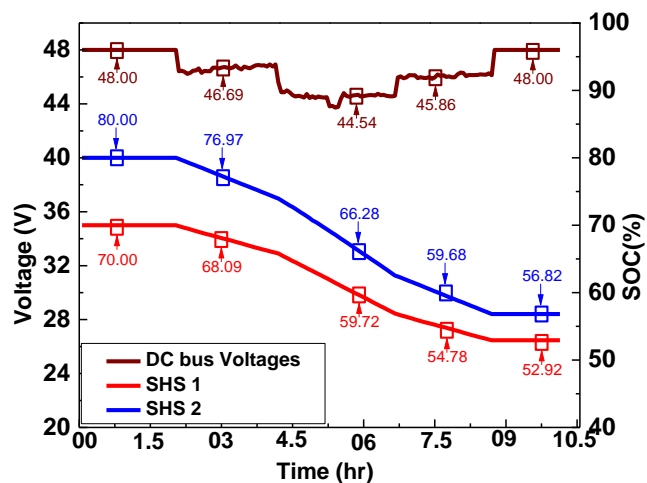

Fig. 9 (b).   DC bus voltage VDC profile (left Y-axis) and SOC variations of various SHS (SOC1 and SOC2) (right Y-axis) at varying communal load demand in case 1 (Hardware results).

At the end of the experiment, the net change in SOC_2 is more than the net change in SOC_1 and resources in both SHS tend to equalize each other. For instance, in Fig. 9 (b), the net change in SOC_2 is 23.12 % and the net change in SOC_2 is 17.08 %. This is because the resource availability in SHS 2 is more than resource availability in SHS 1 as shown by their respective SOC. Although, the speed of equalization can be enhanced using higher values of equalization speed factor α, however in the current scope of the work, the effect of varying α is not considered and it is kept equal to 1 for the current implementation. Overall results show that power contributions in hardware settings are in agreement with simulation results and are in accordance to the proposed droop method such that the SHS with higher resource availability contributes more towards community load demands and overall scheme tends to balance the individual resources in the community.

2) Case 2: SHS having the same installed capacity and same resource Availability

In this experiment, power contributions are assessed for two SHS having same battery capacity, i.e. $C_1 = C_2 = 120$ Ah and similar resource availability, i.e. $SOC_1 = SOC_2 = 80\%$. The results of power contributions I_i^{CL} for communal load demand fulfillment and associated changes in SOC_i are shown in Figs. 10 (a) and 10 (b) respectively. From the results, it is evident that due to identical installed capacity and similar resource availability, both SHS are contributing equal power for the community load applications. Since both the batteries are being discharged at the same rate, their initial and final SOC_i is the same, therefore, their SOC graphs are exactly mapped on each other as shown in Fig. 10 (b). Moreover, the experimental results including power-sharing trends and SOC variations are found in agreement with the simulation results as well as the proposed droop method.
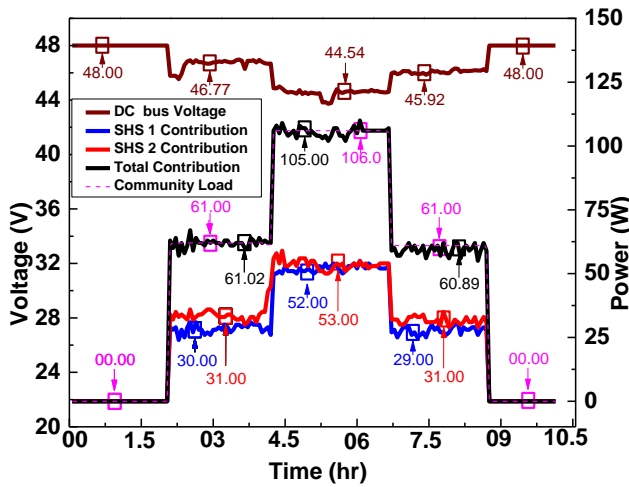

Fig. 8 (a). DC bus voltage V^{DC} profile (left Y-axis) and individual power contributions of various SHS (P_1^{CL} and P_2^{CL}) (right Y-axis) at varying communal load demand in case 2 (Hardware results).
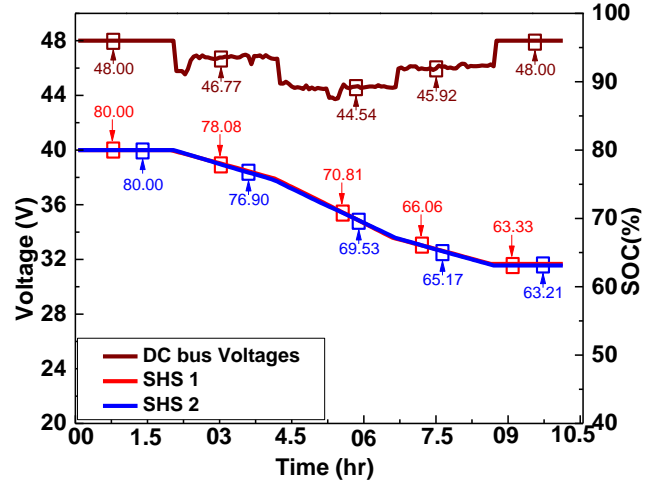

Fig. 8 (b). DC bus voltage V^{DC} profile (left Y-axis) and SOC variations of various SHS (SOC_1 and SOC_2) (right Y-axis) at varying communal load demand in case 2 (Hardware results).

3) Case 3: SHS having the different installed capacity and same resource availability

In this experiment, power contributions are assessed for two SHS having similar resource availability, i.e. $SOC_1 = SOC_2 = 80\%$ with different installed capacity, i.e. $C_1 = 120$ Ah $> C_3 = 800$ Ah. Experimentally achieved power pooling characteristics through the application of the proposed decentralized modified droop control are shown in Fig. 9. Results show that despite having same resource availability, SHS having higher battery capacity, i.e. SHS 1 allows more power to be shared for community load application, in comparison to the SHS 2 having the smaller installed capacity. For instance, to fulfill a communal demand of 109 W in high load demand scenario, SHS 1 is contributing 66 W, while SHS 2 is contributing 42 W. Therefore, hardware results are in accordance to the intended decentralized resource balancing strategy achieved through the modified droop functionality.
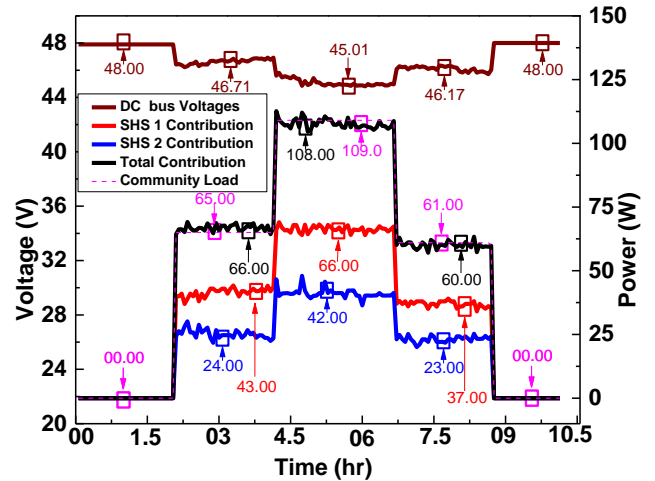

Fig. 9. DC bus voltage V^{DC} profile (left Y-axis) and individual power contributions of various SHS (P_1^{CL} and P_2^{CL}) (right Y-axis) at varying communal load demand in case 3. (Hardware results).

V. CONCLUSION

Solar Home Systems are being largely deployed as a stop-gap measure for providing a very basic level of electrification to off-grid communities. The effective potential of various solar home systems at a village scale can be combined for driving high power community applications. Power electronic interface and decentralized control methodology for the realization of such an integration is presented in this work. A modified droop method based upon the resource availability and installed capacity of the solar home system is proposed for the communication-less coordination among various units of different ratings and capacities. The modified droop based *I-V* droop control ensures the balancing of village resources for the community benefits. The proposed scheme is simulated on MATLAB as well as a hardware prototype is developed in the laboratory. Results show that the proposed scheme enables power sharing and aggregation form multiple solar home systems for community load applications. Moreover, each unit contributes power according to its resource availability as well as installed capacity. Results also highlight that the proposed integration solution is highly beneficial for retrofitting the existing solar home system based electrification implementations for achieving better resource utilization.

REFERENCES

[1] World Energy Outlook (WEO, 2018), Electricity Access Database [Online]. Available: https://www.iea.org/publications/freepublications/publication/WEO2017SpecialReport_EnergyAccessOutlook.pdf

[2] M. Nasir, H. A. Khan, N. A. Zaffar, J. C. Vasquez, and J. M. Guerrero. (Dec, 2018) Scalable Solar dc Microgrids: On the path to revolutionize the electrification architecture of developing communities. *IEEE Electrification Magazine*.

[3] A. Dwi Riana, F. Hunsnayain, E. Andres Pramana, H. Song, P. Yoyok Dwi Setyo, A. Zulfia, *et al.*, "Implementation of talis and dc house system for rural areas in indonesia," *MATEC Web Conf.,* vol. 218, p. 01006, 2018.

[4] R. Bleischwitz, C. Spataru, S. D. VanDeveer, M. Obersteiner, E. van der Voet, C. Johnson, *et al.*, "Resource nexus perspectives towards the United Nations Sustainable Development Goals," *Nature Sustainability,* vol. 1, pp. 737-743, 2018/12/01 2018.

[5] A. Newcombe and E. K. Ackom, "Sustainable solar home systems model: Applying lessons from Bangladesh to Myanmar's rural poor," *Energy for Sustainable Development,* vol. 38, pp. 21-33, 2017.

[6] M. Fowlie, Y. Khaitan, C. Wolfram, and D. Wolfson, "Solar Microgrids and Remote Energy Access: How Weak Incentives Can Undermine Smart Technology," 2018.

[7] M. Nasir, H. A. Khan, A. Hussain, L. Mateen, and N. A. Zaffar, "Solar PV-based scalable DC microgrid for rural electrification in developing regions," *IEEE Transactions on Sustainable Energy,* vol. 9, pp. 390-399, 2018.

[8] C. L. Azimoh, P. Klintenberg, F. Wallin, and B. Karlsson, "Illuminated but not electrified: An assessment of the impact of Solar Home System on rural households in South Africa," *Applied energy,* vol. 155, pp. 354-364, 2015.

[9] H. A. Khan, H. F. Ahmad, M. Nasir, M. F. Nadeem, and N. A. Zaffar, "Decentralised electric power delivery for rural electrification in Pakistan," *Energy policy,* vol. 120, pp. 312-323, 2018.

[10] M. Kurata, N. Matsui, Y. Ikemoto, and H. Tsuboi, "Do determinants of adopting solar home systems differ between households and micro-enterprises? Evidence from rural Bangladesh," *Renewable Energy,* vol. 129, pp. 309-316, 2018/12/01/ 2018.

[11] B. K. Sovacool, "Success and failure in the political economy of solar electrification: Lessons from World Bank Solar Home System (SHS) projects in Sri Lanka and Indonesia," *Energy Policy,* vol. 123, pp. 482-493, 2018.

[12] F. Ahmad and M. S. Alam, "Economic and ecological aspects for microgrids deployment in India," *Sustainable Cities and Society,* vol. 37, pp. 407-419, 2018/02/01/ 2018.

[13] A. Kumar, R. Ferdous, A. Luque-Ayala, C. McEwan, M. Power, B. Turner, *et al.*, "Solar energy for all? Understanding the successes and shortfalls through a critical comparative assessment of Bangladesh, Brazil, India, Mozambique, Sri Lanka and South Africa," *Energy Research & Social Science,* vol. 48, pp. 166-176, 2019/02/01/ 2019.

[14] Q. Shafiee, T. Dragicevic, F. Andrade, J. C. Vasquez, and J. M. Guerrero, "Distributed consensus-based control of multiple DC-microgrids clusters," in *Proc. 40th Annu. Conf. IEEE Ind. Electron. Soc.(IECON)*, 2014, pp. 2056-2062.

[15] X. Lu, K. Sun, J. M. Guerrero, J. C. Vasquez, and L. Huang, "State-of-charge balance using adaptive droop control for distributed energy storage systems in DC microgrid applications," *IEEE Transactions on Industrial Electronics,* vol. 61, pp. 2804-2815, 2014.

[16] Z. Jin, L. Meng, and J. M. Guerrero, "Comparative admittance-based analysis for different droop control approaches in DC microgrids," in *DC Microgrids (ICDCM), 2017 IEEE Second International Conference on*, 2017, pp. 515-522.

[17] M. Nasir, Z. Jin, H. A. Khan, N. A. Zaffar, J. C. Vasquez, and J. M. Guerrero, "A decentralized control architecture applied to dc nanogrid clusters for rural electrification in developing regions," *IEEE Transactions on Power Electronics,* vol. 34, pp. 1773-1785, 2019.

[18] B. Subudhi and R. Pradhan, "A comparative study on maximum power point tracking techniques for photovoltaic power systems," *Sustainable Energy, IEEE transactions on,* vol. 4, pp. 89-98, 2013.

[19] M. Nasir, S. Iqbal, and H. A. Khan, "Optimal Planning and Design of Low-Voltage Low-Power Solar DC Microgrids," *IEEE Transactions on Power Systems,* vol. 33, pp. 2919-2928, 2018.

[20] A. Ausswamaykin and B. Plangklang, "Design of real time management unit for power battery in PV-hybrid power supplies by application of Coulomb counting method," in *2014 International Electrical Engineering Congress (iEECON)*, 2014, pp. 1-4.

[21] M. Hamza, M. Shehroz, S. Fazal, M. Nasir, and H. A. Khan, "Design and analysis of solar PV based low-power low-voltage DC microgrid architectures for rural electrification," in *Power & Energy Society General Meeting, 2017 IEEE*, 2017, pp. 1-5.

[22] R. W. Erickson and D. Maksimovic, *Fundamentals of power electronics*: Springer Science & Business Media, 2007.

[23] F. Gao, S. Bozhko, A. Costabeber, C. Patel, P. Wheeler, C. I. Hill, *et al.*, "Comparative stability analysis of droop control approaches in voltage-source-converter-based DC microgrids," *IEEE Transactions on Power Electronics,* vol. 32, pp. 2395-2415, 2017.

[24] *bPower50, Energy solutions for off-grid households and micro-business.* Available: https://www.bboxx.co.uk/bPower50/